Fracture toughness and failure mechanisms in silica-filled epoxy resin composites: effects of temperature and loading rate

Sung-Wi Koh, Jang-Kyo Kim and Yiu-Wing Mai*
Centre for Advanced Materials Technology, Department of Mechanical Engineering, University of Sydney, Sydney, NSW 2006, Australia
(Received 22 May 1992; revised 23 November 1992)

The fracture toughness and failure mechanisms of epoxy resin composites filled with silica particulates have been investigated in the temperature range −50°C to 80°C and at two loading rates. There are significant effects of temperature and loading rate on impact fracture toughness, which shows a peak at ambient temperature and decreases as temperature is reduced or raised. Fracture toughness under static loading is slightly lower than that of impact loading with similar dependence on temperature. Failure mechanisms are characterized based on SEM examination, which is correlated with the measured fracture toughness, the damage zone size developed at the advancing crack tip, and the residual stresses arising from differential thermal contraction between matrix and particles upon cooling from the cure temperature.

(Keywords: particulate composites; fracture toughness; failure mechanisms; temperature; loading rate)

INTRODUCTION

Particulate-filled polymers are used extensively for medium to high voltage insulating materials due to their superior dielectric strength and high resistivity. The principal materials employed to fabricate particulate composites for such applications are epoxy resins reinforced with inorganic fillers such as silica, alumina, glass beads, etc. Apart from the electrical characteristics of the particulate composites, their mechanical properties, particularly strength, stiffness, fracture and fatigue resistance, and fracture toughness under impact loading conditions, are of paramount importance. A significant amount of information is already available for the fracture behaviour of particulate composites, including silica-filled epoxy resin with which the present study is concerned.

In a series of recent papers[1–5], Nakamura *et al.* have studied extensively the effects of particle size and shape on the mechanical properties and fracture toughness of silica-filled epoxy resin composites, the same materials employed in the present work. They found that for composites filled with angular and spherical particles, the fracture toughness measured from single-edge-notched flexure and double torsion tests increased[1,4] while flexural and tensile strengths decreased[2,5] with increasing particle size in the range 2–47 μm. This behaviour is typical of fracture initiation from particles containing surface flaws and internal defects. The functional dependence of impact fracture toughness on particle size is completely different for different shapes of particles: impact fracture toughness increases with increasing particle size for composites filled with spherical particles[5], whereas the converse is true for those containing angular particles[3]. The elastic moduli are shown to vary only slightly depending on the mode of load application and shape of particles[2,5]: for composites filled with angular particles the flexural and compressive moduli increase marginally whereas the tensile moduli decrease with increasing particle size. The moduli measured in compression, flexure and tension (which is the order of measured values from the highest to the lowest) for composites containing angular particles are always higher than for composites containing spherical particles. In the present study, which is a continuation of the foregoing work[1–5], an investigation has been made on several aspects that have not been studied previously. Special emphasis has been placed on the effects of temperature and loading rate on the fracture behaviour, and in particular the particle–matrix interface related failure mechanisms, of these particulate composites.

EXPERIMENTAL

Materials

The silica-filled epoxy resin composites employed throughout this study were manufactured and supplied by Nitto Denko Co. (Osaka, Japan). The detailed manufacturing procedures have been reported elsewhere[1,4] and are summarized in the following. Two different types of silica particles were used: spherical and angular (or irregular) particles. The spherical silica (SiO_2) particles were obtained by fusing in a flame agglomerated silica which had been produced by hydrolysis of silicon tetrachloride. The angular silica particles were prepared by crushing amorphous silica which had been

* To whom correspondence should be addressed
0032-3861/93/163446-10
© 1993 Butterworth-Heinemann Ltd.

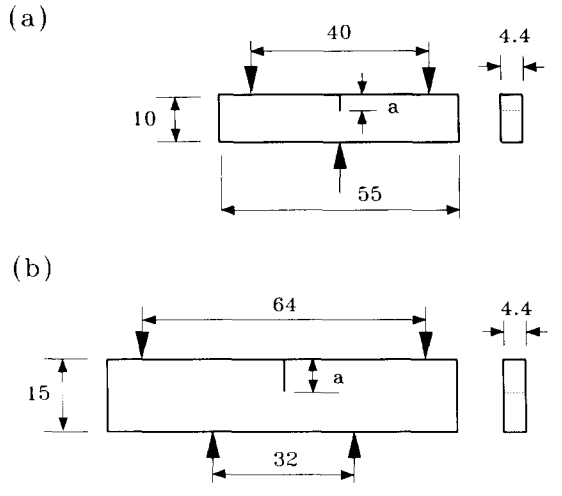

Figure 1 Specimen geometries for (a) Charpy impact and (b) four-point flexure fracture tests

produced by fusing natural raw quartz at 1900°C. The particles were sorted into groups in the range 2–47 μm. The matrix material was prepared with epoxy resin bisphenol A (Epikote 828, Shell Chemical), and 1,2-cyclohexanedicarboxylic anhydride (hardener) and tri-n-butylamine (accelerator) in the ratio of 100:66:0.5 by weight. The mixture of silica particles (296 parts per hundred parts of resin by weight (phr) for a constant weight fraction of 64%) and the matrix material was cured at 120°C for 2 h, followed by post-cure at 140°C for 21 h.

Specimens and tests

The fracture toughness of particulate composites was evaluated under both impact and static loading conditions. The Charpy impact tester was used with a total span $L=40$ mm and a full scale of 0.5 J at a velocity of 2.93 m s^{-1}. Specimens 10 mm wide and 55 mm long were cut from the plates; notches were made in the mid-span and were sharpened further with a razor blade (*Figure 1a*). The initial crack lengths, a, were measured using a profilometer on the fractured specimens after test. The test temperature was varied between −50 and 80°C, which covered the extremes of service temperature of this material, using an environmental chamber. At least eight specimens of different initial crack length, a, were tested for a given set of conditions. The critical potential energy release rate, G_{IC}, was evaluated from the impact energy absorbed, U, using an expression based on the fracture mechanics principles proposed by Plati and Williams[6]:

$$U = U_k + G_{IC}BW\phi \quad (1)$$

where $B(=4.4$ mm) and $W(=10$ mm) are thickness and total width of the specimen, respectively, and the non-dimensional geometric factor, ϕ, is a function of the compliance, C, relative to the ratio of initial crack length to total width, $\alpha(=a/W)$, defined as[6]:

$$\phi = \frac{C}{dC/d\alpha} \quad (2)$$

In a plot of impact energy, U, *versus* $BW\phi$, a least-squares straight line gives a slope which is a measure of G_{IC}, and the vertical intercept represents the kinetic energy loss, U_k, of the fractured sample subjected to impact loading.

Fracture toughness tests were also conducted in static four-point flexure at a cross-head speed of 5 mm min^{-1} and a support span $L=64$ mm (*Figure 1b*). The total width of the specimen was 15 mm and the initial crack length, a, was chosen to maintain the ratio $0.45<\alpha<0.55$. The critical stress intensity factor, K_{IC}, at the onset of crack propagation was calculated from the equation[7]:

$$K_{IC} = \frac{3PL}{4BW^2}\sqrt{\pi a}Y(\alpha) \quad (3)$$

where P is applied stress and the geometric factor $Y(\alpha)$ is given by:

$$Y(\alpha) = 1.122 - 1.121\alpha + 3.740\alpha^2 + 3.873\alpha^3 - 19.05\alpha^4 + 22.55\alpha^5 \quad (4)$$

Four-point flexural tests were also conducted using the same loading configuration as the static fracture tests, except that the specimen thickness was reduced to 4.4 mm.

RESULTS

Impact fracture toughness

Figures 2a and *b* show typical plots of impact fracture energy, U, *versus* $BW\phi$. The slopes of the least-squares lines calculated from equations (1) and (2) give G_{IC} values of 1.1 and 0.94 kJ m^{-2} for composites filled with spherical and angular particles, respectively, with average particle size 6 μm. G_{IC} values determined in this way are plotted as a function of test temperature in *Figures 3a* and *b*. It is obvious that the temperature-dependent impact fracture toughness of filled composites is in general similar to that for (unfilled) epoxy: G_{IC} displays a maximum at ambient temperature and tends to decrease as temperature is increased or reduced further, regardless of the shapes of reinforcing particles. Impact fracture toughness for those with spherical particles is improved by approximately 100% compared with unfilled epoxy: the larger the particle size the greater the improvement (*Figure 3a*). However, the increase in impact fracture toughness is only marginal for composites containing angular particles and becomes almost negligible at the low temperature end (e.g. −50°C).

The effect of particle size on G_{IC} values is clearly shown in *Figures 4a* and *b*, which are replotted from *Figures 3a* and *b*, respectively, for three different test temperatures. It is found that at a given temperature, G_{IC} increases with increasing average particle diameter for a constant weight fraction of spherical particles (*Figure 4a*). However, a similar conclusion cannot be drawn for the composites with angular particles, for which G_{IC} values vary rather irregularly with respect to the particle size, particularly at ambient temperature or above (*Figure 4b*). Moreover, the differences in G_{IC} are much smaller at different temperatures than the composites filled with spherical particles.

Critical stress intensity factor, K_{IC}

The critical stress intensity factor K_{IC} was measured in four-point flexure using equations (3) and (4) for composites filled with the largest particles (i.e. 42 μm for spherical particles and 47 μm for angular particles). To compare these values with those measured in impact loading, the K_{IC} values were also calculated from the known G_{IC} based on the linear elastic fracture mechanics

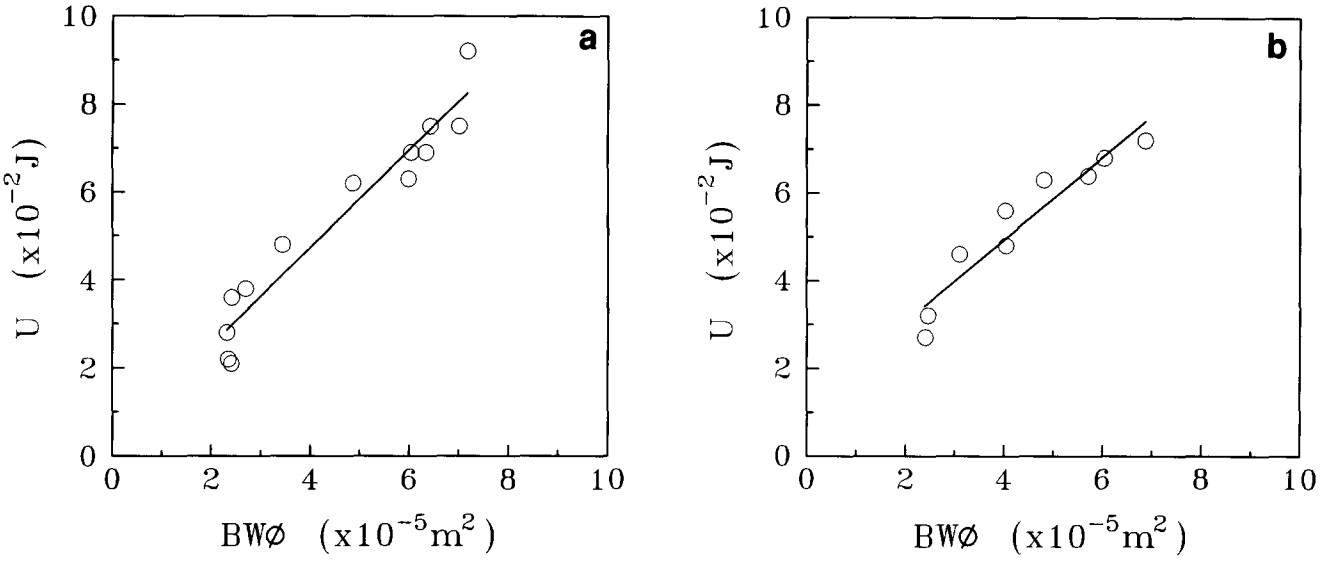

Figure 2 Typical plots of impact energy, U, *versus* $BW\phi$ for composites filled with (a) spherical particles and (b) angular particles. Average particle diameter 6 μm; tested at ambient temperature

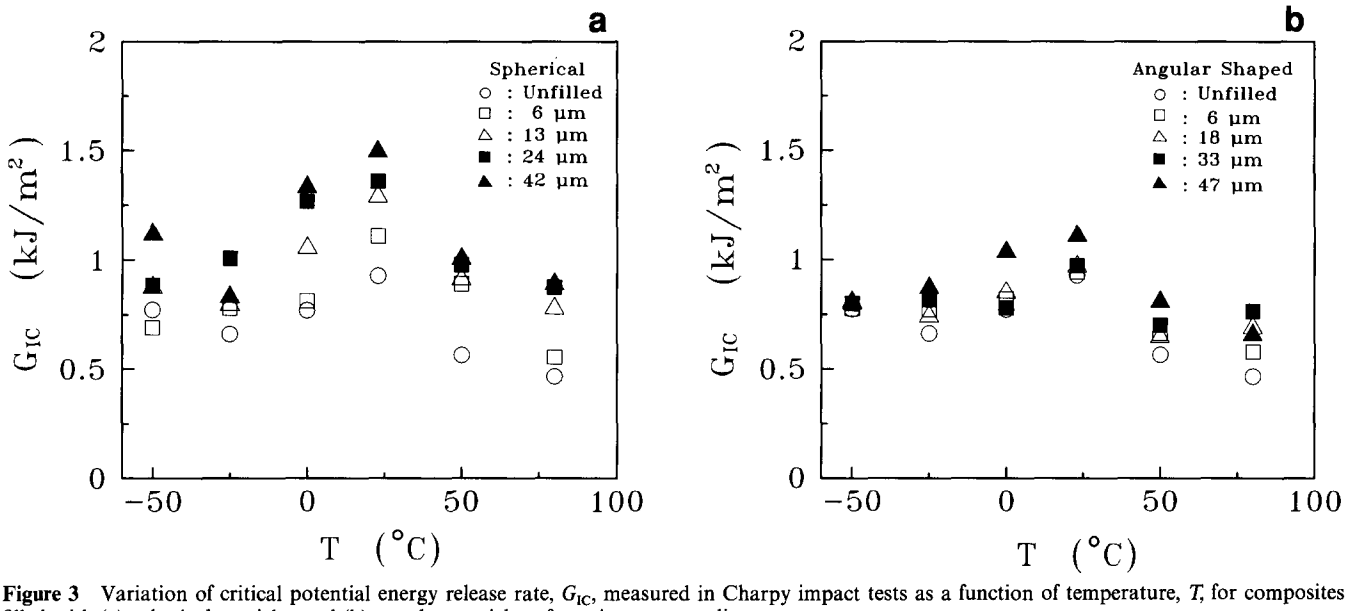

Figure 3 Variation of critical potential energy release rate, G_{IC}, measured in Charpy impact tests as a function of temperature, T, for composites filled with (a) spherical particles and (b) angular particles of varying average diameter

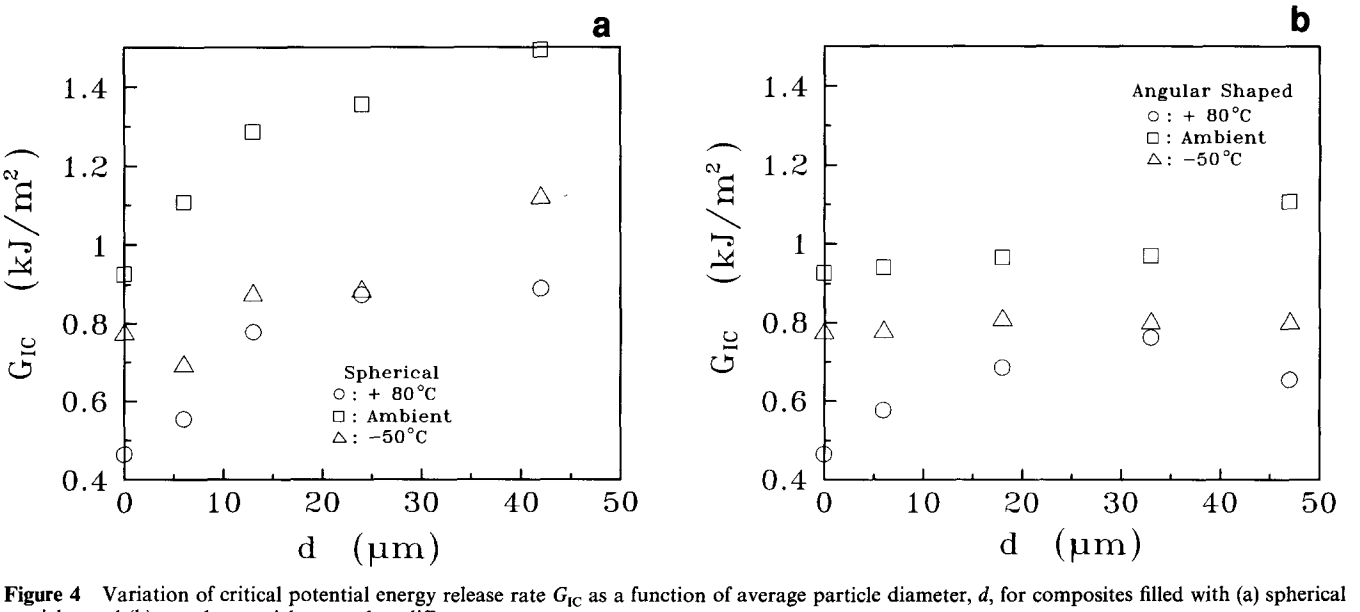

Figure 4 Variation of critical potential energy release rate G_{IC} as a function of average particle diameter, d, for composites filled with (a) spherical particles and (b) angular particles tested at different temperatures

Table 1 Flexural properties and critical stress intensity factors K_{IC}

Properties	Particle shape	Test temperature (°C)		
		−50	23	80
Flexural strength (MPa)	Spherical	128	135	90
	Angular	127	122	112
Flexural modulus (GPa)	Spherical	11.9	13.3	10.5
	Angular	11.5	11.3	10.5
K_{IC} (static flexure) (MPa $m^{1/2}$)	Spherical	3.33	3.72	2.97
	Angular	3.18	3.55	2.86
K_{IC} (Charpy impact) (MPa $m^{1/2}$)	Spherical	3.87	4.72	3.24
	Angular	3.21	3.75	2.78

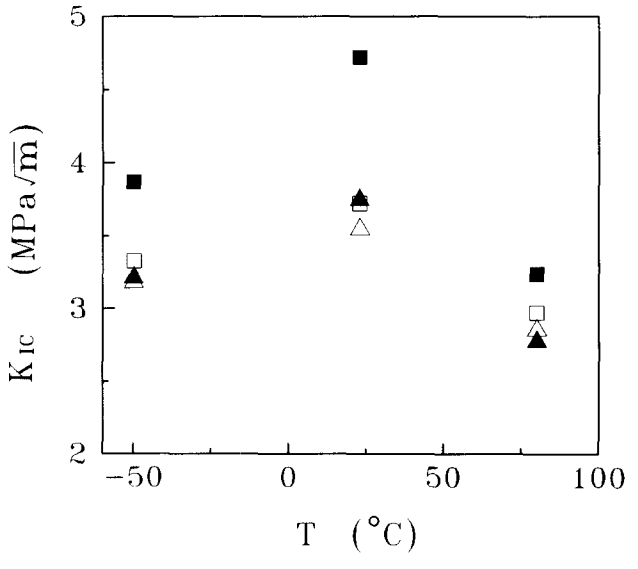

Figure 5 Variation of critical stress intensity factor K_{IC} as a function of test temperature, T, for composites filled with 42 μm spherical particles (■, □) and 47 μm angular particles (▲, △). K_{IC} determined in Charpy impact tests (■, ▲) and in static four-point flexure (□, △)

(LEFM) equation:

$$K_{IC} = \sqrt{\frac{G_{IC}E}{(1-\nu^2)}} \tag{5}$$

where E is the elastic modulus and ν (=0.33[4]) is the Poisson ratio of the composite material. To a first approximation, E is taken from the flexural modulus measured in static flexure of unnotched specimens. Any variation in E which might have been caused by viscoelasticity of the epoxy resin at different loading rates (i.e. impact *versus* static loading) is neglected here. This approximation is deemed reasonable in view of the finding by Kinloch *et al.*[8] that elastic modulus of a similar bisphenol A epoxy resin does not vary much (i.e. less than 8% increase at the most at −60°C) and becomes almost constant at temperatures higher than −20°C when the strain rate is increased from $\dot{\varepsilon}=10^{-5}\,s^{-1}$ to $10^{-2}\,s^{-1}$ in unidirectional compression. In the present study, the nominal strain rates calculated according to the simple beam theory (i.e. $\dot{\varepsilon}=6Wv/L^2$ and $\dot{\varepsilon}=2.18Wv/L^2$, respectively, for three-point and four-point bending, where v is the loading or striking speed) give $\dot{\varepsilon}=0.11\,s^{-1}$ and $1.95\times10^{-4}\,s^{-1}$ for Charpy impact and four-point static flexure, respectively. These values fall within the range of strain rates used in the above work[8]. A maximum 8% increase in E will result in only a 4% increase in K_{IC}, which would hardly alter the general trend of the results. Further, for a composite containing ceramic particles of weight fraction as high as 64% (or equivalent volume fraction about 51%), it is most likely that the strain rate dependence of elastic modulus will become less significant.

A summary of the experimental results for flexural properties and the critical stress intensity factors for different temperatures and particle shapes is given in *Table 1*. The slightly lower values of flexural strength and elastic modulus at 80°C compared to those measured at lower temperatures are a direct influence of the substantial loss of strength and stiffness near the glass transition temperature (~100°C). These mechanical properties are almost constant within the data scatter at other temperatures. K_{IC} values determined from static and impact fracture tests are compared as a function of temperature in *Figure 5*. The general trend of temperature dependence of K_{IC} for a given particle shape is basically similar for both loading conditions: K_{IC} shows a maximum at ambient temperature and tends to decrease with increasing or reducing temperature. K_{IC} values are always higher for the composites containing spherical particles than for those with angular particles at a given temperature. The difference in K_{IC} measured in static flexure between the composites with two different shapes of reinforcing particles are much smaller than those obtained from impact fracture tests.

Scanning electron microscopic examination

The major failure mechanisms of these composites are studied based on the SEM examination of the fracture surfaces. Typical impact fracture surfaces of the composites filled with spherical particles (of average diameter 42 μm) are shown in *Figure 6* from which progressive changes in the locus of failure can be clearly identified as a result of change in test temperature for a given loading condition. In *Figures 6a* and *b*, which were tested at −50°C, the silica particle surface appears to be relatively clean with tiny epoxy nodules distributed uniformly. The locus of failure is not exactly at the equator of the sphere but is significantly above it. However, there is spatial continuity at the particle–matrix interface without apparent debonding. In contrast to the foregoing phenomenon, specimens tested at ambient or above (*Figures 6c*, *d* and *e*) display epoxy patches of substantial thickness covering almost the entire particle surface. The locus of failure has moved further up to the pole of the sphere and the fracture appears to be completely through the matrix material. In addition, there are significant changes in the morphology of the matrix fracture surface: at −50°C the fracture through the epoxy matrix appears to be relatively brittle without much deformation as might be expected, but it becomes significantly more ductile as the temperature is increased. Therefore, it can be rationalized that the failure in this composite under impact loading tends to be more matrix-controlled with increasing temperature. In general, the silica particle–epoxy matrix interface appears to be well bonded and does not allow extensive debonding under impact conditions even though brittle fracture is, to a certain extent, enhanced at the low temperature end.

Apart from the foregoing failure mechanisms, another distinctive feature is identified for specimens tested at low temperature (e.g. −50°C) under impact loading. Some

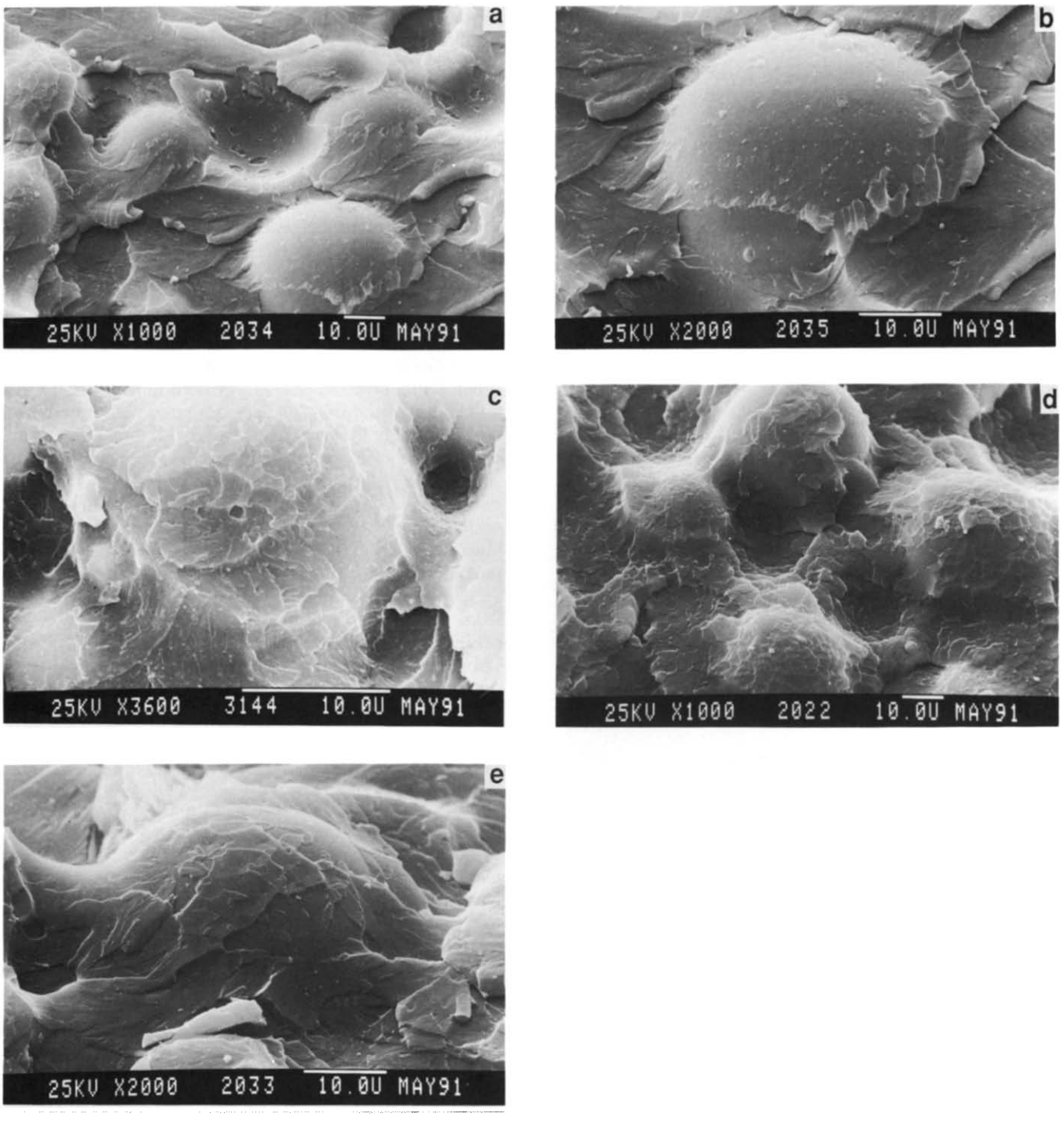

Figure 6 SEM photographs of impact fracture surfaces for spherical particle composites tested at (a) and (b) −50°C; (c) 23°C; (d) and (e) 80°C

particles have been fractured into halves as shown in *Figure 7*, due probably to pre-existing external flaws and/or internal defects generated in the particles during the manufacturing process, as suggested by the non-uniform distribution of the broken particles. This observation is valid only near (i.e. within approximately 500 μm from) the initial crack tip for composites filled with large particles. However, there is no discernible discontinuity at the particle–matrix interface (*Figure 7b*) supporting the foregoing conclusion of strong interfacial bonding. Composites containing smaller particles do not show particle fractures, suggesting that a significant size effect is present.

Typical impact fracture surfaces for composites filled with angular particles are shown in *Figure 8*. There are few differences between surface morphologies of specimens tested at different temperatures, supporting the experimental results that the fracture toughness is not influenced significantly by test temperature for this composite (*Figure 3b*). A large number of fractured particles are shown in *Figures 8a* and *c*, showing that angular particles are more susceptible to fracture than spherical particles. There is, however, spatial continuity between fractured particles and epoxy resin (*Figure 8b*). Smearing of matrix material onto the particles is also shown in *Figure 8d*, particularly at temperatures higher

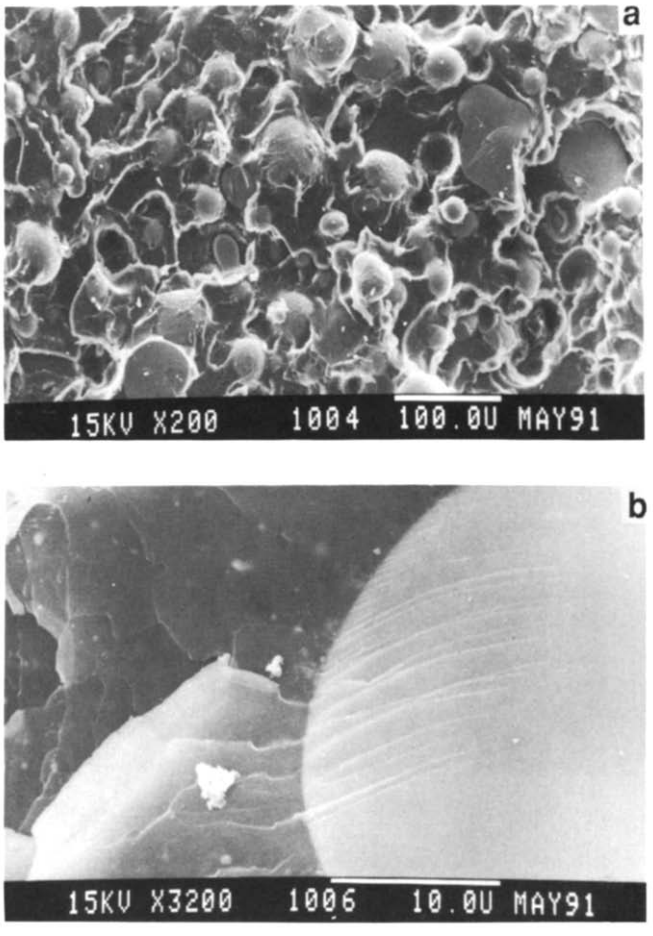

Figure 7 SEM photographs of impact fracture surfaces for spherical particle composites tested at (a) and (b) −50°C, showing the fractured particles

than ambient, if the major plane of the particle is favourably oriented against the advancing crack tip. These observations confirm that the inherent bonding at the particle–matrix interface is strong.

The main difference between the fracture surfaces of composites tested under impact and static loading conditions is the occurrence of debonding at the particle–matrix interface in the case of static loading. No discernible interfacial debonding has been observed at any temperature for the impact fracture surfaces, though there are some relatively clean surfaces of exposed particles, particularly for specimens tested at the low temperature end, as mentioned above. In contrast, apparent debonding is prevalent near the initial crack for specimens tested under static loading, as shown in a series of SEM photographs taken across the specimen depth in *Figure 9*. Depending on the position of the particles relative to the advancing crack tip, some particles are pulled out completely leaving clean hemispherical holes, while other particles are debonded from the matrix with distinct interfacial cracks. The length of the debonded region, which is the distance between the initial crack tip and the farthest debonded particle as measured from the microphotographs, is approximately 500, 280 and 240 μm for the specimens tested at −50, 23 and 80°C, respectively. It is noted that these values are far less than 10% of the total unbroken ligament area of specimen cross section before fracture. Associated with the interfacial debonding near the initial crack tip is the brittle fracture of the matrix material between reinforcing particles without significant shear deformation, particularly at low temperatures (*Figure 9a*).

DISCUSSION

Effect of temperature

The temperature dependence of impact fracture toughness for pure epoxy resins and silica-filled composites (*Figure 3a*) has a significant analogy with the results reported[9] on pure and rubber-modified epoxy resins. Both systems exhibited a large peak in impact fracture toughness at ambient temperature which dropped off rapidly with further increase or decrease in test temperature. It was shown that thermal blunting of the advancing crack tip caused by adiabatic heating under impact loading condition[10] had increased the resistance to crack propagation as a result of localized high effective temperature (corresponding to the sum of the test temperature and the adiabatic temperature rise). A 'stretched zone' near the initial crack tip was given as evidence of thermal blunting in the pure and rubber-modified epoxy resins[9]. However, without any solid physical evidence it is difficult to confirm that the same thermal blunting mechanism is also operative in the composites employed in the present study. Further, even if this mechanism was present under favourable conditions, its beneficial effect would be far smaller in the composites than in the pure or rubber-modified epoxy resins. In fact, the thermal blunting mechanism requires the correct degree of temperature rise to be effective for improving the fracture toughness.

The parabolic decrease in fracture toughness at temperatures higher and lower than ambient may be related to the detrimental effects of softening of the matrix material and the residual thermal stresses, respectively. It is already demonstrated that strength and stiffness are reduced significantly at high temperatures above ambient (*Table 1*). Therefore, the beneficial effects of toughening mechanisms that may be operative at these high temperatures are outweighed by the loss of strength and stiffness, resulting in a substantial reduction in fracture toughness.

The differential thermal expansion is a very important parameter in a composite which in turn determines the residual stress distribution and thus has vital effects on the resultant mechanical performance. When the differential thermal expansion coefficient ($\Delta\alpha = \alpha_m - \alpha_p$) between the matrix ($\alpha_m$) and the particle ($\alpha_p$) is positive, as in the case of the silica-filled epoxy resin composites, a radial compressive stress is generated at the particle–matrix interface upon cooling from the cure temperature. When there are large compressive radial stresses at the interface, the surrounding matrix will be subjected to a residual tensile stress in the circumferential direction which decreases the capability of the matrix material to sustain crack initiation. A crude estimate of the magnitude of these residual stresses in the radial (σ_r) and circumferential (σ_t) directions can be made from[11]:

$$-\sigma_r = 2\sigma_t = \frac{\Delta\alpha\Delta T}{(1+v_m/2E_m)+(1-2v_p/E_p)} \approx \Delta\alpha\Delta T E_m \quad (6)$$

where E and v are elastic modulus and Poisson ratio, respectively. The subscripts m and p refer to the matrix and particle, respectively. For the silica-filled epoxy resin

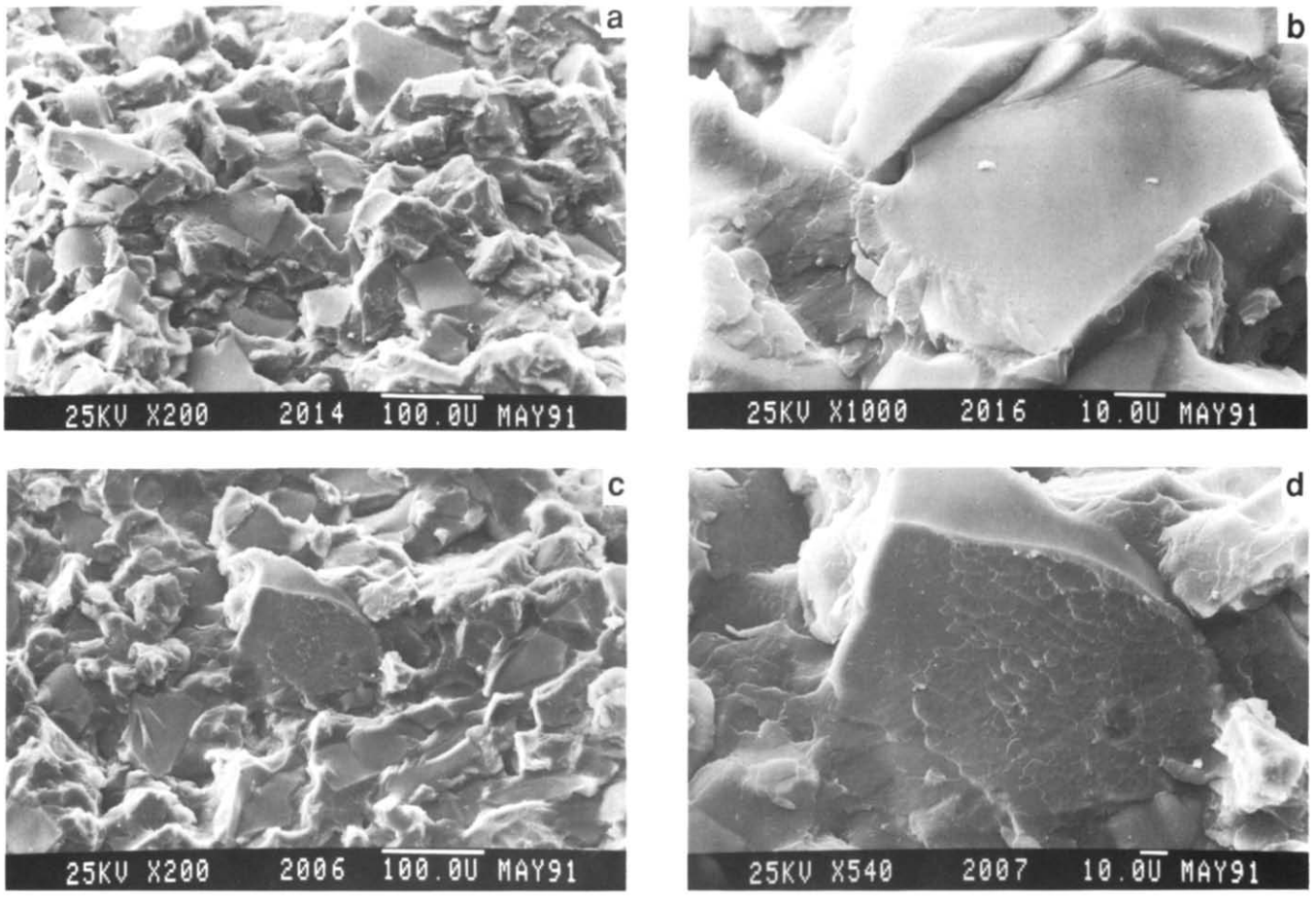

Figure 8 SEM photographs of impact fracture surfaces for angular particle composites tested at (a) and (b) −50°C; (c) and (d) 23°C

composites both $\Delta\alpha$ ($\approx 50\times10^{-6}$ to $60\times10^{-6}\,°C^{-1}$)[12] and the temperature difference upon cooling $\Delta T(\approx 100°C)$ are positive so that $-\sigma_r = 2\sigma_t \approx 50$ MPa at ambient temperature. It is obvious then that these residual stresses will increase (in absolute terms) with further decrease in temperature below zero.

The presence of large differential thermal residual stresses mentioned earlier, which increase with decreasing temperature, has an adverse effect on the composite fracture toughness (*Table 1* and *Figure 3*). While the radial compressive stress enhances, to a certain extent, the mechanical bonding which provides an efficient stress stransfer across the particle–matrix interface, it certainly has a detrimental effect in triggering catastrophic unstable crack propagation initiating from flaws and/or imperfections which the particles may contain. Particle fractures are more likely to occur under high residual stresses at low temperatures (*Figures 7a* and *b*), resulting in a planar fracture surface. In addition, the tensile circumferential stresses developed around the particles further promote brittle fracture due to a lower strain required for crack initiation.

The temperature-dependent failure mechanisms occurring around the particle–matrix interface (*Figure 6*) can be explained in terms of the inherent interfacial bond strength, τ_b, relative to the matrix shear strength, τ_m. This idea has been applied successfully to the fibre-reinforced epoxy matrix composites[13]. If τ_b is significantly lower than τ_m, adhesive failure at the particle–matrix interface (i.e. interfacial debonding) is predominant regardless of test temperature. In other words, the interface-controlled failure mechanism is affected little by the test temperature. In contrast, if τ_b is higher than τ_m, i.e. there is strong interfacial bonding as is the case of the materials employed in the present study, failure at the interface region is mainly cohesive and the temperature dependence is matrix-controlled due to changes in matrix strength and stiffness.

It has been noted that there are progressive changes in the locus of failure as a result of changes in test temperature (*Figure 6*). When the temperature was varied from −50°C to 80°C, the line dividing the two distinct regions of particle surface morphology (i.e. exposed particle surface with little bonded matrix material and the region smeared predominantly by the matrix material) moved towards the pole of the particle. There are also significant variations in the morphology of the matrix material, suggesting changes in the matrix deformation (from brittle to ductile) with increasing temperature. This observation is analogous to the morphology changes due to different particle surface conditions. Following the early work on fractography and failure mechanisms of several different particle-filled epoxy resin composites[14–17], Miller *et al.*[18] provided comprehensive pictures on the interface-related failure mechanisms of polyethylene composites filled with glass spheres having a range of different surface treatments. Depending on the level of surface treatment of the glass spheres, failure is typically adhesive and progressively changing towards cohesive. For the composites containing glass spheres with no surface modification, there is no substantial bonding at the particle–matrix interface and the locus of failure is

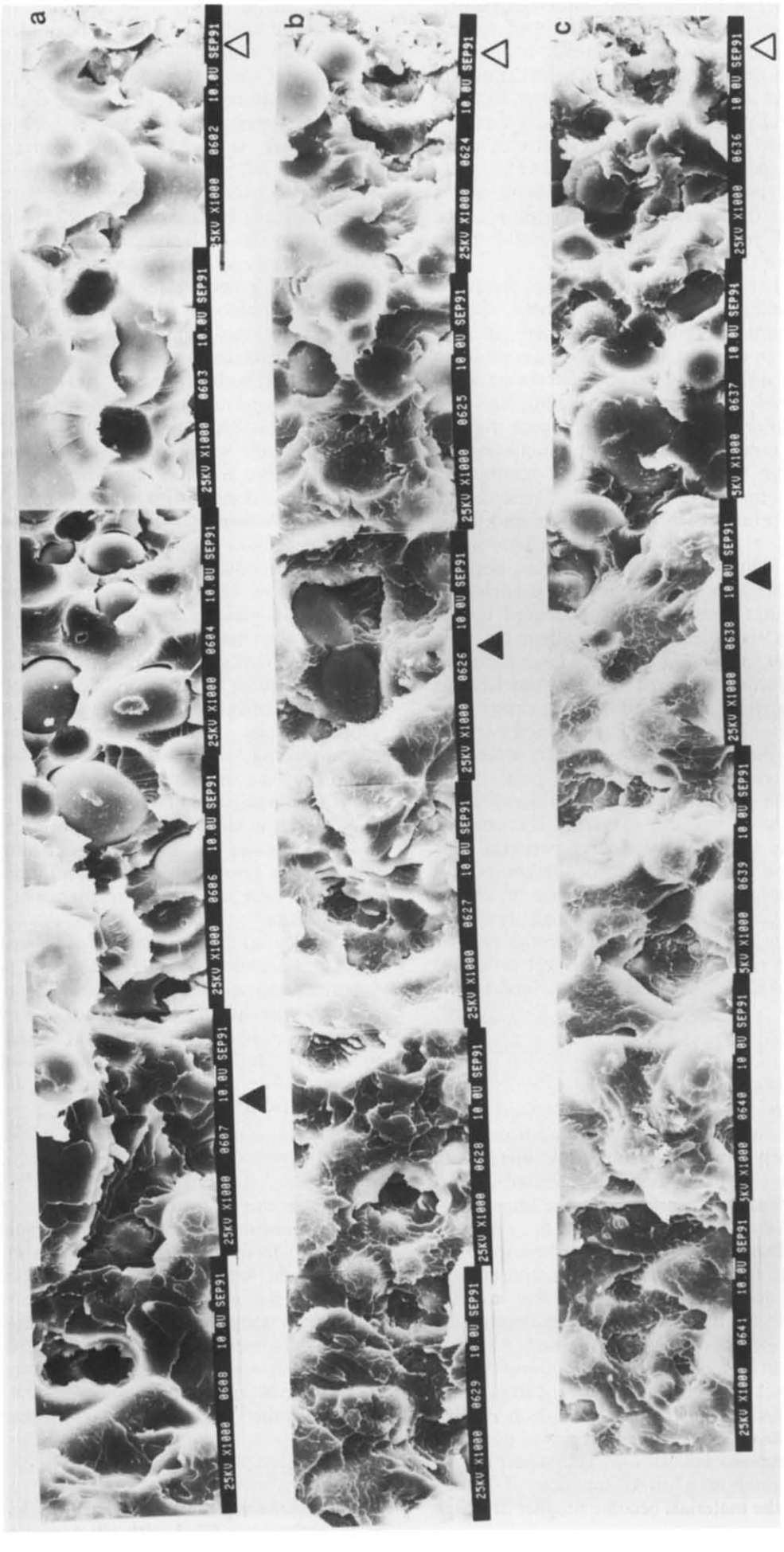

Figure 9 Series of SEM photographs of static flexure fracture surfaces for spherical particle composites of average diameter 42 μm tested at (a) -50°C, (b) 23°C and (c) 80°C, showing the debonded particles near the initial notch. △ and ▲ *indicate the initial crack tip and the length of the particle–matrix interface debonded region, respectively*

at the equator of the spheres with associated brittle fracture in the matrix. At the highest level of surface modification, the locus of failure has moved to the pole of the glass spheres and is completely through the matrix material. These microscopic examinations seem to agree well with analytical predictions by Guild and Young[19] in a combined finite element and spatial statistics study on particulate composites. They[19] found that for poorly bonded particles the position for maximum stress concentration is at the equator of the spheres as is the case of spherical holes[16], whereas for well-bonded particles it is above the pole of the spheres.

It is found that some particles have fractured under impact loading over almost the whole fracture surface for the composites filled with angular particles (*Figures 8a* and *c*). In contrast, for composites containing spherical particles, only limited particle fracture occurred near the initial crack tip under impact loading and at a low temperature (*Figure 7a*). Since the impact fracture toughness of the former composites (containing angular particles) is always lower than the latter (containing spherical particles) for a given condition of particle size and test temperature (compare *Figures 3a* and *b*), it appears that particle fractures do not contribute much to the fracture toughness of these composites. Because the strengths of both spherical and angular particles are greater than the matrix material (as evidenced by the higher strength of the filled composites than the pure epoxy[2,5], except for those filled with very large particles) it is believed that surface flaws and internal imperfections inherent in the particles are most likely the causes that trigger premature particle fractures. For spherical particles well bonded to the matrix in particular, since the maximum direct stress occurs near the pole of the particles[19], particle fracture means a significant stress concentration in the particle due to defects. It is obvious then that it is easy to find flaws in large particles. This is why flexural and tensile strengths of the composites containing particles of both shapes decrease invariably with increasing particle size[2,5]. The high tendency of particle fracture in composites containing angular particles is in part related to the large aspect ratio and irregular shape of the particles which causes a large tensile stress to build up.

Effect of loading rate

The significantly higher K_{IC} values obtained under impact loading compared to those obtained from static flexure, particularly for the composites filled with spherical particles (*Figure 5*), can be attributed in part to the dynamic effects associated with the impact test method[20,21]. The dynamic effects include the relatively high contact stiffness of the impact striker–specimen interface compared to that of the specimen, and the loss and regaining of contact between the striker and the specimen due to the specimen accelerating and decreasing relative to the striker during impact loading. All these effects result in an increasing number of oscillations observed in the force–deflection record of the impact test as the impact velocity is increased[22]. Kinloch *et al.*[22] showed that the measured fracture energies of pure and rubber-modified epoxies are strongly dependent on the time to failure, which is a direct function of impact velocity, and that the materials become tougher at a high impact velocity.

The particle–matrix interface debonding observed under static loading conditions has a detrimental effect on fracture toughness since it deteriorates the full capability of the matrix material for shear deformation due to premature failure. It is shown that there is a small region of apparent particle–matrix debonding near the initial crack tip when tested under static flexure (*Figure 9*) followed by a rough region of matrix deformation over the majority of the fracture surface. In fact, a similar observation has been reported in a series of papers by Cantwell and co-workers[23–25] on silica- and alumina-filled epoxy resin composites. They reported that there are in general three distinct regions of different fracture morphologies: (i) the area surrounding the defects or next to the initial crack tip shows extensive particle–matrix debonding, representing the region of slow and subcritical crack growth; (ii) the region surrounding (or next to) the subcritical region exhibits a flat featureless appearance; (iii) the rough region or fast fracture region which covers the majority of fracture surface exhibits a strong three-dimensional appearance, this being associated with extensive crack tip deflection. They[23–25] showed that the relative size of the individual region depended strongly on the strain rate: specimens tested at a loading rate between 1.0 and 50 mm min^{-1} did not show any sign of particle–matrix debonding without a significant change in fracture toughness. In contrast, specimens tested at a very slow loading rate (e.g. 0.1 mm min^{-1}) had a substantial decrease in fracture toughness with a large region of debonded particles near the initial precrack, suggesting that the crack had propagated in a subcritical manner over a distance corresponding to the fracture process zone or damage zone. They showed that the debonding process ahead of the crack tip degraded the toughness of the material and might result in the premature failure of the specimen. In this case, instead of promoting toughening mechanisms, the particles provoked isolated fractures in the damage zone and hence reduced the resistance of the material to gross failure[26]. Therefore, the presence of debonded particle degrades the resistance of the local material to crack propagation because the cracks deflect into the debonded material at the poles of the particles[27]. The damage zone shown by Nakamura *et al.*[1,4] encompasses at least several particle diameters at a load corresponding to 80% of the fracture load. The damage zone size, s, present before unstable catastrophic fracture can be estimated from the Dugdale model[28]:

$$s \approx \frac{\pi}{8}\left(\frac{K_{IC}}{\sigma_y}\right)^2 \tag{7}$$

where σ_y is the yield strength of the material. Taking, to a first approximation, the flexural strength for σ_y and K_{IC} values in *Table 1*, this gives approximately 266, 298 and 428 μm for the composites containing spherical particles tested at -50, 23 and 80°C, respectively. These predictions should be compared to the lengths of the actual debonded region (i.e. 500, 280 and 240 μm, respectively) measured from the fracture surfaces. The discrepancies are probably due to the inaccuracy in estimating the yield strength σ_y from the flexural tests.

SUMMARY

The fracture toughness and failure mechanisms of epoxy resin composites filled with silica particulates (of both

spherical and angular shapes at a constant weight fraction of 64%) were investigated at varying temperatures and loading rates. Impact fracture toughness for the spherical particle composites was improved by approximately 100% compared to the pure epoxy: the larger the particle size the greater the toughness for a given temperature. The temperature dependence of impact fracture toughness for filled composites was generally similar to that for the pure epoxy, namely that fracture toughness showed a peak at ambient temperature and decreased as the temperature was raised or reduced further. The static fracture toughness determined from three-point flexure showed a similar temperature dependence, but with slightly lower values (20–30%) compared to the impact fracture toughness. The effects of low temperature on fracture toughness were explained in terms of thermal residual stresses caused by the differential thermal contraction between the particles and the matrix upon cooling from the cure temperature, while the loading rate dependence was related to the dynamic effects of the impact tests and the particle–matrix debonding near the initial crack tip.

Fracture analysis conducted using scanning electron microscopy showed that the impact fracture surfaces for spherical particulate composites were characterized mainly by shear yielding of the matrix material between reinforcing particles and smearing of the resin around the pole of the particle depending on the crack location and test temperature. The main difference between impact and static fracture surfaces was the occurrence of debonding at the particle–resin interface. No discernible interfacial debonding was observed at any temperature for the impact fracture surfaces, though some relatively clean particle surfaces were found at a low temperature. In contrast, obvious debonding was prevalent particularly near the initial crack tip for the static fracture surfaces. This implied that slow loading rates promoted interfacial debonding of otherwise well-bonded particles, which caused a reduction in the resistance of material to gross failure. The debonded length measured on the fracture surface was of the same order of magnitude as the damage zone size predicted based on the Dugdale model. Particle fracture itself contributes little to the composite fracture toughness since this failure mechanism is caused mainly by inherent defects present in the particles. In conclusion the major failure mechanisms are matrix shear yielding between the particles and crack tip deflection which generates a large fracture surface area.

ACKNOWLEDGEMENTS

The authors thank Dr Yoshinobu Nakamura of Nitto Denko Co. (Osaka, Japan) for supplying the materials for testing. The use of facilities in the Electron Microscopic Unit of the University of Sydney is much appreciated. S. W. K. was a Visiting Scholar from the National Fisheries University of Pusan, Korea to the Department of Mechanical Engineering at the University of Sydney when this work was performed.

REFERENCES

1 Nakamura, Y., Yamaguchi, M., Kitayama, A., Okubo, M. and Matsubo, T. *Polymer* 1992, **32**, 2221
2 Nakamura, Y., Yamaguchi, M., Okubo, M. and Matsubo, T. *J. Appl. Polym. Sci.* 1992, **44**, 151
3 Nakamura, Y., Yamaguchi, M., Okubo, M. and Matsubo, T. *Polymer* 1991, **32**, 2976
4 Nakamura, Y., Yamaguchi, M., Okubo, M. and Matsubo, T. *Polymer* 1992, **33**, 3415
5 Nakamura, Y., Yamaguchi, M., Okubo, M. and Matsubo, T. *J. Appl. Polym. Sci.* 1992, **45**, 1281
6 Plati, E. and Williams, J. G. *Polym. Eng. Sci.* 1975, **15**, 470
7 Murakami, Y. 'Stress Intensity Factors Handbook', Pergamon Press, Oxford, 1988
8 Kinloch, A. J., Shaw, S. J. and Hunston, D. L. *Polymer* 1983, **24**, 1355
9 Low, I. M. and Mai, Y. W. *J. Mater. Sci.* 1989, **24**, 1634
10 Williams, J. G. and Hodgkinson, J. M. *Proc. R. Soc. Lond.* 1981, **A375**, 231
11 Selsing, J. *J. Am. Ceram. Soc.* 1961, **44**, 419
12 Ibrahim, I. A., Mohamed, F. A. and Lavernia, E. J. *J. Mater. Sci.* 1991, **26**, 1137
13 Kim, J. K., Baillie, C. and Mai, Y. W. *Composite Sci. Technol.* 1992, **43**, 283
14 Roulin-Moloney, A. C., Kausch, H. H. and Stieger, H. R. *J. Mater. Sci.* 1983, **18**, 208
15 Roulin-Moloney, A. C., Kausch, H. H. and Stieger, H. R. *J. Mater. Sci.* 1984, **19**, 1125
16 Spanoudakis, J. and Young, R. J. *J. Mater. Sci.* 1984, **19**, 473
17 Spanoudakis, J. and Young, R. J. *J. Mater. Sci.* 1984, **19**, 487
18 Miller, J. D., Ishida, H. and Maurer, F. H. J. *J. Mater. Sci.* 1989, **24**, 2555
19 Guild, F. J. and Young, R. J. *J. Mater. Sci.* 1989, **24**, 298
20 Kalthoff, J. F. *Int. J. Fracture* 1985, **27**, 277
21 Williams, J. G. and Adams, G. C. *Int. J. Fracture* 1987, **33**, 209
22 Kinloch, A. J., Kodokian, G. A. and Jamarani, M. B. *J. Mater. Sci.* 1987, **22**, 4111
23 Roulin-Moloney, A. C., Cantwell, W. J. and Kausch, H. H. *Polym. Composites* 1987, **8**, 314
24 Cantwell, W. J., Roulin-Moloney, A. C. and Kaiser, T. *J. Mater. Sci.* 1988, **23**, 1615
25 Cantwell, W. J., Smith, J. W. and Kausch, H. H. *J. Mater. Sci.* 1990, **25**, 633
26 Evans, A. G., Williams, S. and Beaumont, P. W. R. *J. Mater. Sci.* 1985, **20**, 3668
27 Smith, J. W., Kaiser, T. and Roulin-Moloney, A. C. *J. Mater. Sci.* 1988, **23**, 3833
28 Williams, J. G. 'Fracture Mechanics of Polymers', Ellis Horwood/John Wiley, Chichester, 1984